VICTORIA UNIVERSITY
MELBOURNE AUSTRALIA

bushfire&natural HAZARDSCRC

bnhcrc.com.au

PHYSICS-BASED SIMULATION OF FIREBRAND AND HEAT FLUX ON STRUCTURES IN THE CONTEXT OF AS3959

Amila Wickramasinghe, Nazmul Khan, Khalid Moinuddin
Victoria University and Bushfire & Natural Hazards CRC

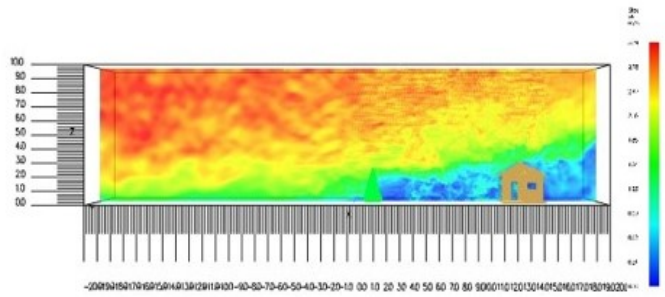

(a)

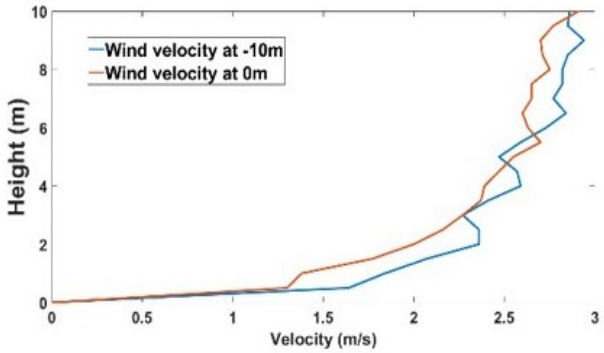

(b)

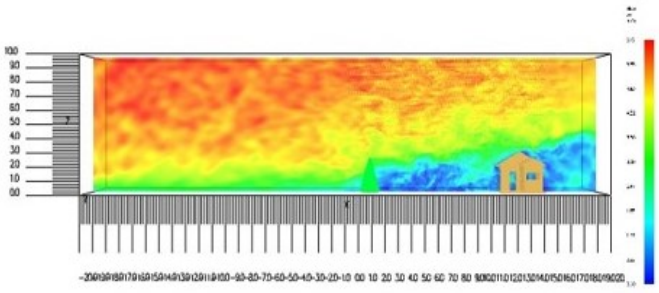

(c)

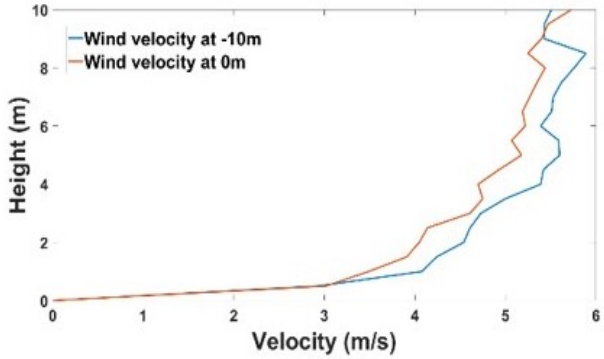

(d)

Version	Release history	Date
1.0	Initial release of document	02/04/2020

Australian Government
Department of Industry, Science, Energy and Resources

Business Cooperative Research Centres Program

Publisher:
Bushfire and Natural Hazards CRC

April 2020

Citation: Wickramasinghe A, Khan N, Moinuddin K (2020) Physics-based simulation of firebrand and heat flux on structures in the context of AS3959, Bushfire and Natural Hazards CRC, Melbourne.

Cover: The smokeview representations of wind flow respectively. Synthetic eddy methodology is used to introduce turbulence at the domain inlet.

TABLE OF CONTENTS

ABSTRACT

Firebrand is known as one of the most dangerous airborne components of wildfires having the potential to ignite structures in Wildland-Urban Interface (WUI). Quantifying the firebrand and heat flux on structures is essential to determine the wildfire risks and prepare strategic plans to mitigate the hazard. We endeavor to use a physics-based model, Fire Dynamic Simulator (FDS) to map firebrand and heat flux to determine the vulnerability of structures in WUI. In this study, we have validated FDS' tree burning and firebrand transporting sub-models against the experiment conducted in no wind condition at the National Institute of Standards and Technology (NIST). The experimental data of firebands were processed to use as inputs in the numerical simulation and the grid convergence was appraised in terms of mass loss rate (MLR). The intial velocity and direction of firebrands, the number of generations were determined as model inputs by a reverse analysis through comparing firebrand distribution with the experiment. As the FDS' sub-models were validated, we attempted to quantify the heat flux and firebrand risk on a structure at three different driving wind velocities. Increasing wind speed showed more firebrands transported towards the structure but none of them landed on the house because of the low height of the tree and insufficiency of fire-induced buoyancy to lift them enough to carry a longer distance by the wind field. Similarly, heat flux computed on the structure is well below Australian building standard AS3959's bushfire attack level (BAL). it is due to the low heat release by single tree burning instead of a 100m wide fire line assumed in the standard. In future study, simulations will be conducted with a cluster of taller trees (100m wide) to quantify the heat flux and firebrand hazard on structures to apprise AS3959.

INTRODUCTION

Wildifre attack mechanisms could be classified into direct flame contact, radiant heat, firebrand attack or a combination of them [2, 3]. Firebrands could be igniting barks, leaves, twigs and, nuts originated from burning vegetation. The firebrand generation and transportation vary mainly by vegetation type, humidity (RH), temperature, and wind conditions. Spot fires could occur once firebrands landed on a fuel bed or a combustible part of a structure. Fire intensity, moisture content, characteristics of vegetation and wind velocity determine the firebrand tearing off from vegetation while their size, shape, wind condition can vary the spotting distance [4, 5].

The composition and configuration of vegetation and fuel bed determine the combustion and heat release of wildfires [6]. The vegetation type and their thermo-physical parameters may cause variations in the number of firebrand generation and their physical and thermal characteristics. Experiments carried out by Filkov et al [7] and Manzello et al [8] demonstrate different vegetations like Douglas fir, Pitch pine, Korean pine, etc produce firebrands of various sizes, mass, and shapes. The moisture content of the fuel is an important parameter for the production of firebrands [4, 9].

Physics-based model has been used to investigate the physical mechanisms of fire behaviour including tree burning [10-13]. Fire Dynamics Simulator (FDS) is a physics-based model developed by NIST for structure fire modelling. FDS uses computational fluid dynamics method to solve governing equations for buoyant flow, heat transfer, combustion, and thermal degradation of vegetative fuels [14]. This model is based on the Large Eddy Simulation (LES) framework to account for turbulence and can introduce Lagrangian particles which can be used to represent firebrands. The model consists of Lagrangian particle tracking schemes to resolve the firebrand transportation, size and mass distribution, momentum and energy transfer to and from particles of complex objects that cannot be solved on the numerical grid [15].

Australian Standard AS3959-2018 [16] is the prescription of the construction of buildings in bushfire-prone areas to supplant AS3959-2009 and 1999 [2, 16]. The primary objective is to prescribe a suite of protections for building occupants and buildings to withstand a bushfire attack. According to the standard, the firebrand risk in WUI is increasing(qualitatively) with the Bushfire Attack Level (BAL) thresholds. The level of radiant heat flux is used as the basis for the range of bushfire attack levels in AS3959 [16]. Vegetation type, up or downslope, distance from the site to classified vegetation and Fire Danger Index (FDI) - [the numerical explanation of the severity of bushfire] are taken into account when determining the BAL [2, 16].

The first phase of this project is validating the data on firebrands mass and size distribution following the Douglas fir tree burning experiment conducted at NIST [9]. In this NIST experiment, the tree was dried to the average moisture content of 10% before burned in no wind condition [9]. Mass of the tree was measured as the time progressed after the ignition. Firebrands were collected placing water-filled pans at strategic locations based on a series of scoping experiments [9]. The number of generated firebrands, their directions and velocities were unknown. One objective of this validation is to find these unknowns.

In the second phase, Pyrosim software [17] is used to design a house with proper architectural features and wind fields of U10 (wind velocity at 10 m high from the ground in an open field) = 3 m/s, 6 m/s, and 12.5 m/s are added to examine the firebrand landing on the designed house as well as heat flux. The number of firebrands generated by a burning tree, their initial velocity and direction are taken as inputs from the first phase. The goal of this phase is to quantify firebrand and heat flux on the designed structure.

METHODOLOGY

VALIDATION OF TREE BURNING AND FIREBRAND TRANSPORT

FDS' particle transport model is validated by firebrand mass and size distribution from burning Douglas fir tree. Such firebrand mass and size (length and diameter) data are available from the laboratory experiment conducted at NIST. We categorized these firebrands into 30 classes based on their mass. The length and diameter of each mass class are used as inputs in the numerical modelling. The total mass of collected firebrands and, burner details were taken from the experiment [9]. The time series of mass loss of the tree fire modelling is validated against the experimental data first. Thermo-physical parameters used in this modelling are presented in Table 1 as per Moinuddin et al [13], Mell et al [10], and McGrattan et al [18]. Mechanisms of firebrand production/tear-off and firebrands burning will not be investigated in this model.

Parameters	Moisture	Vegetation	Char
Thermal conductivity (W/m K)	2.0	2.0	2.0
Specific heat capacity (kJ/kg K)	4.184	1.2	1.2
Density (kg/m^3)	1000	514	300
Reference temperature (°C)	100	200	-
Refrence rate	0.002	0.0005	-
Heating rate (°C/min)	1.6	1.6	-
Conductivity (W/m K)	2.0	2.0	2.0
Heat of reaction (kJ/kg)	2500	418	-
Mass fraction	0.1	0.9	-

TABLE 1 – THERMAL PARAMETERS USED IN DOUGLAS FIR TREE BURNING FDS MODEL (10, 13, 19)

The tree geometry is taken as a cone shape having a height of 2.6m and girth of 1.5m, same as the original tree. The area of the domain determined according to the toal area needed to place FDS devices to represent firebrand collecting pans. Domain height was determined by visual observation of flame (represented by heat release rate per unit volume isosurfaces) height through the FDS companion software, Smokeview. All flames must be captured within the domain. Therefore, a domain 8m x 8m x 10m has been used for the simulations. Figure 1(a) shows a snapshot of Smokeview with X and Z domain sizes and the tree is located at (0, 0, 0) coordinates of the XYZ plane. The base height of the tree is 0.15m relative to the bottom plane.

(a (b

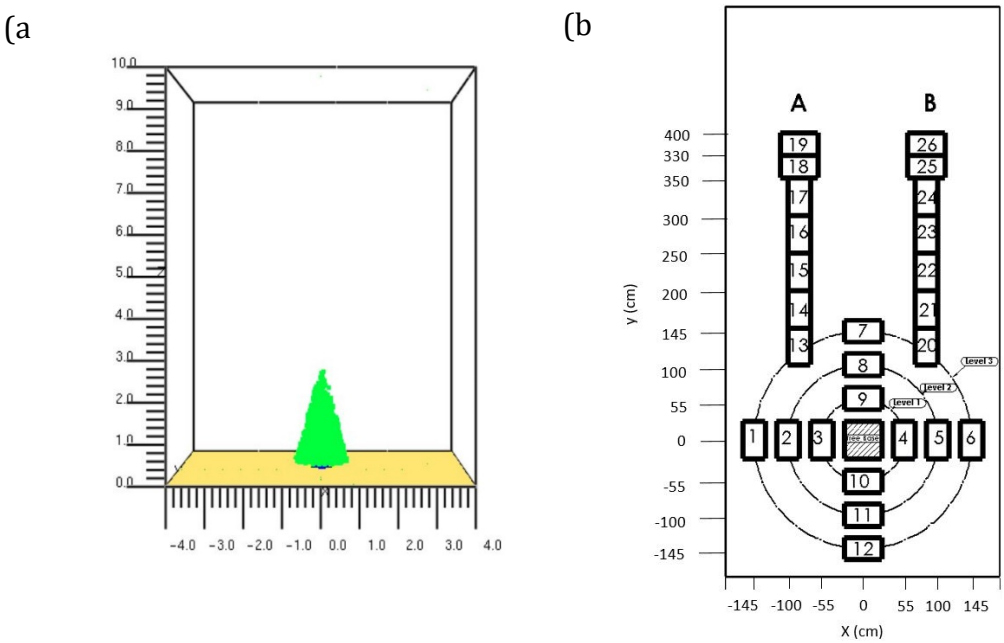

FIGURE 1(A) IS A SMOKEVIEW REPRESENTATION OF MODEL TREE (AT 0 SECONDS) WITH X, Y DOMAIN SIZES. THE PLAN VIEW OF FIREBRAND COLLECTION PAN ARRANGEMENT IS SHOWN IN (B). EACH PAN HAS BEEN NUMBERED 1 TO 26 AND THE TREE BASE IS AT THE MIDDLE OF 1-6 AND 7-12 PAN SERIES. A, B ARE THE PARALLEL ARRANGEMENT. PANS WHICH OBTAINED FIREBRANDS ARE IN CIRCULAR LEVELS OF 1, 2 AND, 3.

The burnable mass of the tree consists of needles and two different types of twigs. The diameters and mass fractions of the fuel elements measured in the laboratory experiment are presented in Table 2. Mass per volume (MPV) input parameters of the model have been calculated by dividing the individual component mass by a total tree volume of 1.53m^3. The length of the burnable mass was taken as 0.1m as per [19]. The moisture content of the fuel was taken as 10% of the same as the laboratory experiment.

Fuel	Diameter (mm)	Mass fraction (%)	MPV (kg/m^3)
Needles	0-6	65	4.208
Twigs (type 1)	0-6	17.5	1.133
Twigs (type 2)	6-10	17.5	1.133

TABLE 2 – COMPOSITION AND PHYSICAL PROPERTIES OF BURNABLE FUEL OF DOUGLAS FIR TREE MEASURED AT NIST

Firebrand data (mass and size) of the Douglas fir tree burning experiment were categorized into 30 mass classes. These classes are ranging from 0.005g to 2.00g and the numbers of firebrands falling into each mass class are known. Figure 2(a) presents the firebrand number in each mass class and Figure 2(b) shows the diameter and length of firebrand vary with the mass class. Out of collected firebrand particles, 97% is less than 1g. When the mass is increased the number of generated firebrands is decreased. The highest number of firebrands (27) are in the 0.02g mass class. There are about 60% of firebrands which have a length of less than 50 mm and diameter less than 3.7 mm. The maximum firebrand length and diameter are 140 mm and 7.4 mm respectively.

(a)

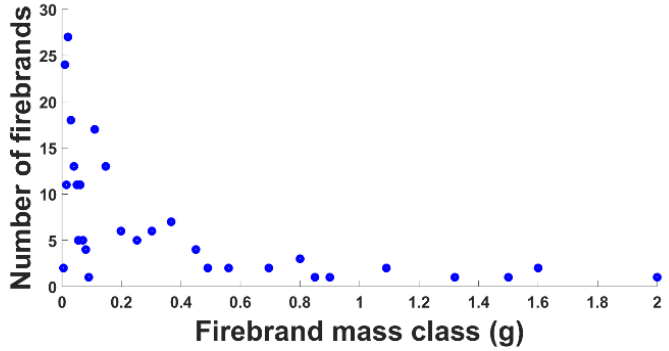

(b)

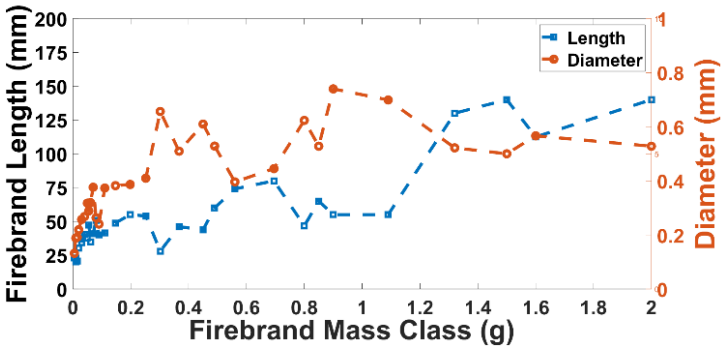

FIGURE 2(A) ILLUSTRATES THE NUMBER OF FIREBRANDS IN EACH MASS CLASS AND THE NUMBER IS REDUCING WITH HIGHER MASS CLASSES. LENGTH AND DIAMETER OF FIREBRANDS SHOW INCREASING PATTERN MOVING TOWARDS HIGHER MASS CLASSES IN (B).

Firebrands are released throughout the volume of the model tree. Tree burning almost completed after 30 seconds in the laboratory experiment [9]. Therefore, the firebrand generation time is maintained for 30 seconds. Total simulation time is kept as 45 seconds to provide sufficient time to land firebrands on the ground surface. There is no wind flow and firebrands move and settle under the fire-induced buoyancy and gravity. The default 'cylinder' drag law of FDS is being used for firebrands to replicate the drag force on their movement. Firebrand inserting time interval is being set to manipulate the inserting number of firebrands according to each mass class. Pans are represented by setting rectangular shape devices in FDS to measure accumulated firebrand landing mass.

Domain discretizing by appropriate grid (cell) size is significant in quantitative numerical analysis and results should be grid-converged [13]. Therefore, the grid convergence analysis is carried out for 100 mm, 75 mm, 50 mm and 37.5 mm grid cells in terms of mass loss rate (MLR) and heat release rate (HRR). The multiplications of the total number (70) of collected firebrands [9] are used as inputs to the models as the number of firebrand generation during the burning. We are carrying out an inverse analysis by inputting number, direction and the velocity of firebrands to obtain them on pans in 1, 2, 3 levels and A, B parallel series. As shown in Table 3, the collected number of firebrands is multiplied by 2, 3, 4, and 5 times in different simulations as the input of generation.

Case	Generated firebrands		Velocity and directions	
	Number	Mass(g)	Vertical (cm/s)	Radial (cm/s)
Laboratory experiment	unknown	unknown	unknown	unknown
Simulation 1(50mm grid)	2×70	23.23	5	0
			10	30
			60	180
			70	210
Simulation 2(50mm grid)	3×70	34.85	5	0
			10	30
			60	180
			70	210
Simulation 3(50mm grid)	4×70	46.46	5	0
			10	30
			60	180
			70	210
Simulation 4(50mm grid)	5×70	232.31	5	0
			10	30
			60	180
			70	210

TABLE 3 – NUMBER, VELOCITY AND DIRECTION OF FIREBRAND VARIATIONS TO OBTAIN MATCHING COLLECTIONS

With each variation of generation number, eight different directions and different velocity combinations are being used. Once we obtained firebrands on pans in level 1, 2, 3, etc. by giving different velocity combinations, used that velocity combination (vertical and horizontal components) as the initial velocity of firebrands. After ejecting with this velocity firebrands are subject to the influence of buoyancy induced by fire and the gravity force to be transported to the places where they land. Burning a tree forms an updraft convective column and according to Koo et al. [20] the firebrand is acted by the gravity force that occurred by its own weight and the pressure force induced by the flow around the firebrand. Since wind is not applied in this experiment, the lift force becomes the pressure force.

Each firebrand class has different a length and a diameter so that the variations of projected area results different drag forces on firebrands by the instant fire-induced flow. This determines the changes in firebrand movements and their distribution around the tree. The total average mass of collected firebrands in the laboratory experiment is 18 g. Firebrand generation number has been changed in the numerical simulation to obtain the average total firebrand mass collection on trays as in laboratory experiment. In this study, we changed the generation number as multiplications (4, 5, 6) of collected firebrands of 70.

FIREBRAND AND HEAT FLUX ON A STRUCTURE

In this phase, we are aiming to simulate the heat flux and firebrand landing on a designed house. The input number, direction and, velocities of firebrands are taken from the first phase. The structure is designed with proper architectural features such as walls, doors, windows, roofs using Pyrosim software[17]. Wind

fields of U10 = 3 m/s, 6 m/s and, 12.5 m/s are added to examine the firebrand landing on the designed house. The buoyancy for firebrand transporting is generated by modelling a Douglas fir tree burning.

(a

(b

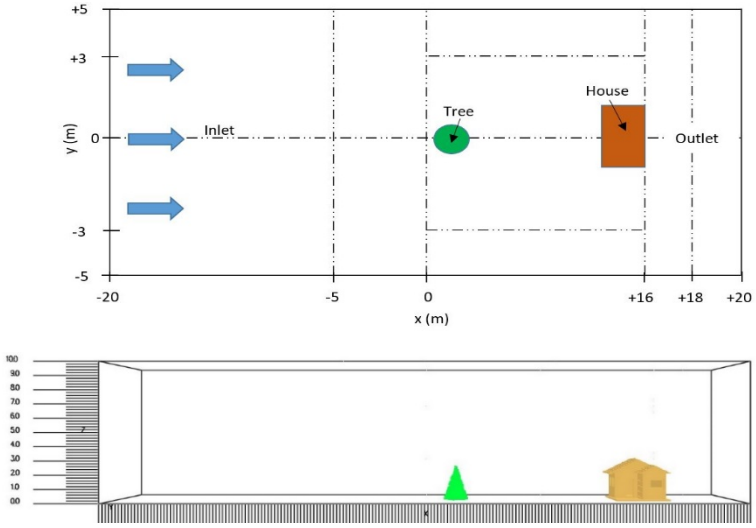

FIGURE 3(A) PLAN VIEW OF THE SIMULATION DOMAIN. AREA (16 M×6 M×10 M) OF TREE BURNING AND FIREBRAND TRANSPORTING HAS FINEST GRID RESOLUTION OF 50MM. THE DISTANCE BETWEEN VEGETATION AND THE HOUSE IS 10 M. (B) IS THE GRAPHICAL REPRESENTATION OF DOMAIN IN SMOKEVIEW WHERE TREE AND HOUSE SITUATED AT 2 M AND 12 M DISTANCE IN POSITIVE X DIRECTION.

The simulations are being performed over a domain that is 40 m long, 10 m wide and 10 m high. From the inlet to 20 m, there are two a non-burning subdomain with 200 mm and 100 mm grid sizes, followed by a 6 m □ 16 m area where the tree and house are located. The burning and firebrand transportation mainly happen in this sub-domain and the grid size is taken as 50 mm. The aspect ratio is being kept as 2 when moving from one domain to another. The plan view of the domain is shown in Figure 3(a) and a snapshot of smokeview presented in Figure 3(b).

The distance between the tree and the house is taken as 10 m which is the minimum flatland distance of BAL40 for forest vegetation in AS3959 [2, 16]. The wind flow at the domian inlet maintains a log profile with velocities of 3 m/s, 6 m/s and 12.5 m/s at 10 m above the ground level (U_10). Synthetic eddy methodology (SEM) is used to introduce turbulence at the domain inlet as proposed by Jarrin et al [21]. The flow is run for 60 seconds until to obtain a quasy-steady wind flow before starting the ignition and firebrand generation. Devices are set in between area of the house and tree to collect data about firebrand number and landing mass. The particle flux on the house is measured though a vertical plane at +12 m distance. The radiation heat fluxes are computed at strategic locations of the designed house such as door corners, wall corners, gutters, three levels of the roof etc, by setting heat flux devices available in FDS. The aim is to examine MLR, HRR, heat flux on house, firebrand distribution and landing on the house in different wind velocities.

RESULTS AND ANALYSIS

In Figure 4 the MLR and HRR results are presented from simulations with various grids. The MLR and HRR profiles are shifted to keep peaks roughly aligned to make the comparison easier in Figure 4(b) and (d).With decreasing grid size, results gradually convergence. The results with 50 and 37.5 mm grids are closely matched. Therefore 50 mm grid size can be considered reasonable to use in this tree burning simulation. The total mass loss (kg) and heat loss (kJ) from simulations with each grid size are also presented.

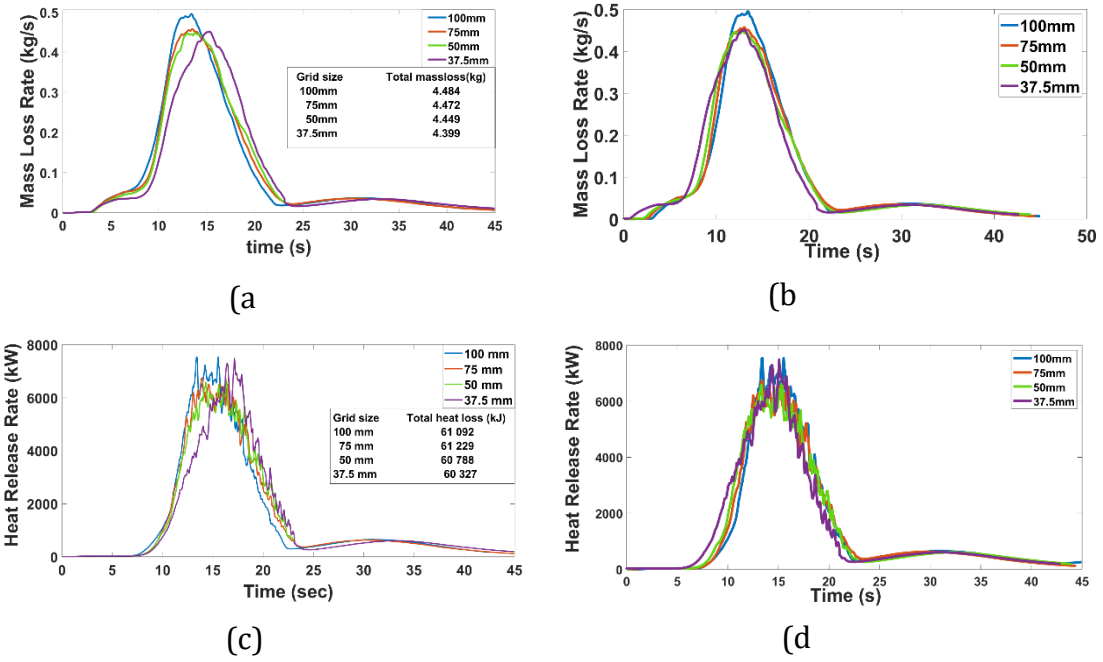

FIGURE 4(A) COMPARISON OF MASS LOSS RATE (MLR) RESULTS FOR 2.6 M DOUGLAS FIR TREE SIMULATIONS FOR GRID SIZE 100 MM, 75 MM, 50 MM AND, 37.5 MM. (B) MLR RESULTS AFTER PEAK SHIFTING. (C) COMPARISON OF HEAT RELEASE RATE (HRR) FOR GRID SIZE 100 MM, 75 MM, 50 MM AND, 37.5 MM. (D) HRR RESULTS AFTER PEAK SHIFTING.

Figure 5 shows the comparison of experiment and simulation results obtained using a 50 mm grid. Simulation is reasonably close to the experiment and the difference in total mass loss is about 8.5%. Peak mass loss rate of the experiment is 0.417kg/s where simulation shows it as 0.447 kg/s which is a 6.7% difference. The shapes of the two curves are qualitatively-similar. Here the experimental MLR profile was shifted to align with simulation for better comparison.

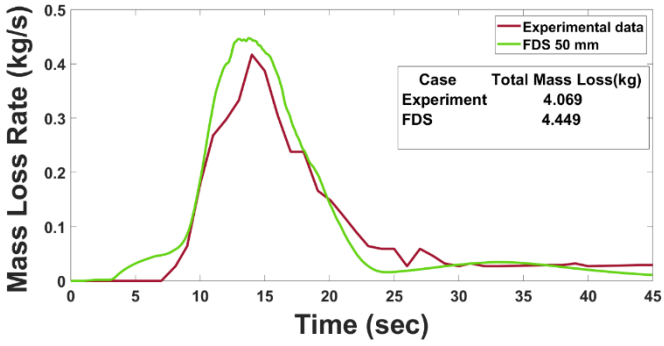

FIGURE 5. MLR COMPARISON OF EXPERIMENT AND FDS 50 MM GRID SIZE. THE SHAPE OF THE TWO CURVES ARE REASONABLE. SIMULATION RESULTS SHOW HIGHER TOTAL MASS LOSS DURING THE SIMULATION TIME OF 45 SECONDS.

Preliminary results show that giving horizontal and vertical initial velocities of 10 cm/s and 30 cm/s could get firebrands only from the nearest four pans (Level 1) around the tree. When these velocities multiply by factor of 2, up to 20 cm/s and 60 cm/s keeping the same ejecting angle (71.50) to the vertical axis, level 2 of pans (refer to Figure 1(b)) also received some firebrands. The mass of firebrands received by the nearest pans (3, 4, 9, 10) to the tree base has reduced with this velocity increment. At the same time, some firebrands have shifted to 2, 4, 8 and 11 pans in level 2. Increasing vertical and horizontal velocities up to 70 cm/s and 210 cm/s could obtain firebrands from the third level of pans and even on pans in A, B parallel series. When giving velocities of 70 cm/s vertically and 210 cm/s horizontally caused moving more firebrands towards the third level of pans while reducing the mass on first and second level compared to the lower velocities of 10-30 cm/s and 20-60 cm/s. Horizontal and vertical velocity components of 70 cm/s and 210 cm/s are the minimum velocity components that could obtain firebrands in pans at all three levels and in parallel A and B pan arrangements. This velocity and direction are taken as input for the next set of simulations. Figure 6 represents the smokeview visual output of tree burning at different times and firebrand distribution with 70-210 cm/s initial particle velocity.

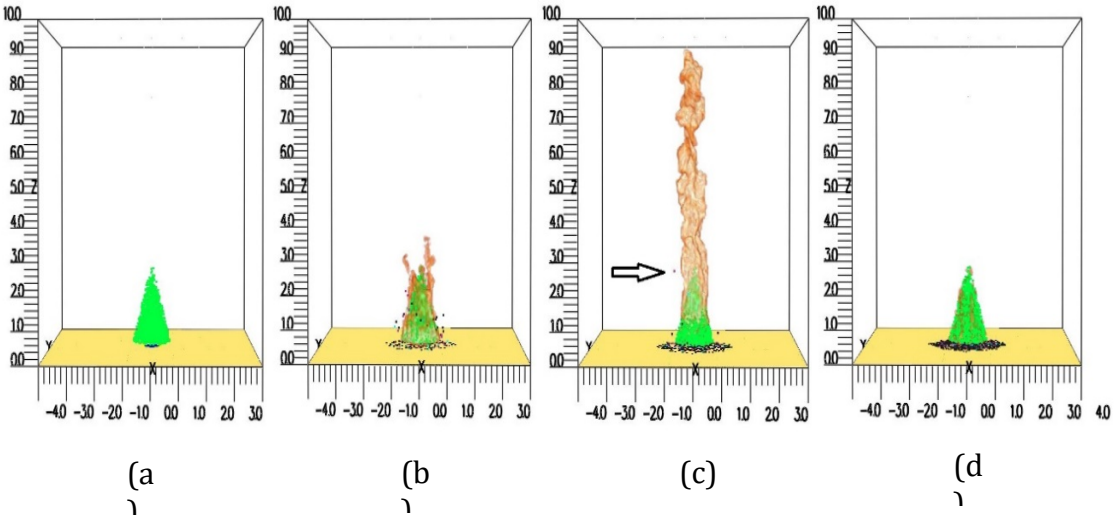

FIGURE 6 – GRAPHICAL REPRESENTATION OF DOUGLAS FIR TREE BURNING AND FIREBRAND DISTRIBUTION AT (A) ZERO SECOND (B) 14 SECONDS (C) 20.7 SECONDS AND (D) 35 SECONDS. THE ARROW IN FIGURE 6(C) SHOWS SOME FIREBRANDS MOVING UPWARDS WITH THE CONVECTIVE COLUMN DURING THE INTENSIVE BURNING BEFORE LANDING ON THE FLOOR.

The total firebrand mass collected from the pan arrangement of the laboratory experiment was 18±4 g. The number of firebrands generated from the tree was changed in each simulation to obtain 18±4 g while keeping 70 cm/s-210 cm/s velocities and direction fixed. The input number has been changed according to the multiplications of original firebrands (70) collected in the experiment. Table 4 shows the simulation cases ran with different input number of firebrands, inserted and collected mass and, the numbers of pans which received firebrands. It shows that inserting 70□5 amount of firebrands could obtain 18.904 g of firebrands in the pans under the influence of fire-induced buoyancy and gravity.

Case	Number of firebrands	Mass (g)		Firebrands receeivng pans
		Inserted	Collected	
1	70x4	66.80	16.45	1 to 12, 13 and 14
2	70x5	86.92	18.90	1 to 12, 13 and 14
3	70x6	99..40	26.36	1 to 12, 13 and 14

TABLE 4 – MASS RECEIVED BY PANS INPUTTING DIFFERENT NUMBER OF FIREBRANDS

The firebrand mass distribution contour map of case-2 is presented in Figure 7. The mass distribution of firebrands around the tree is not uniform. The mass of the firebrands landed in the positive x-direction ishigher than the negative x-direction. The positive y-direction has also received more firebrand mass than negative y-direction. This may be because of the random characteristics of fire-induced instant buoyancy. The maximum mass of firebrands obtained by a pan is around 3g.

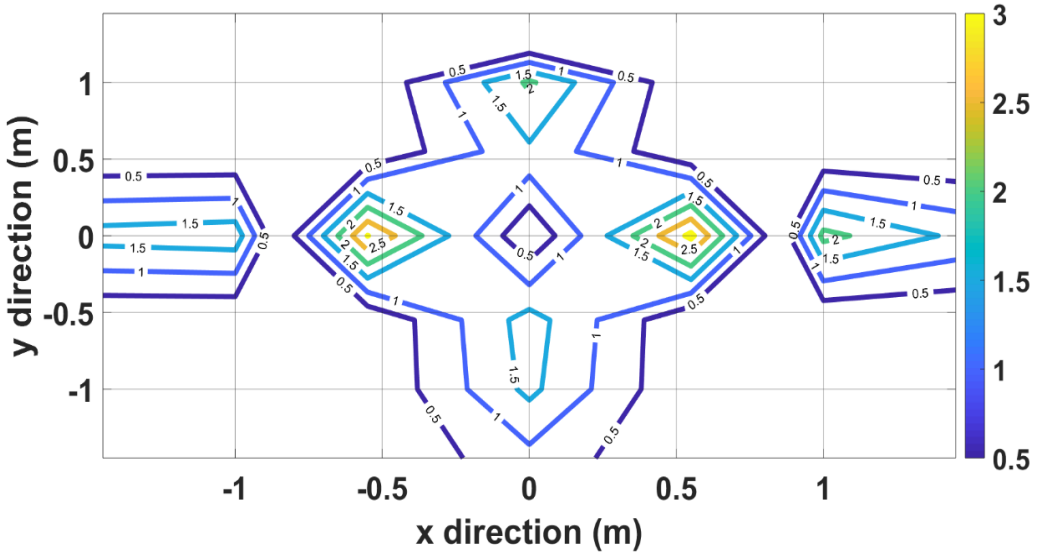

FIGURE 7 – CONTOUR MAP OF FIREBRAND DISTRIBUTION AROUND THE TREE IN 70-210CM/S VELOCITY. AT (X, Y) = 0,0 POINT IS THE BASE WHERE TREE IS MOUNTED. THIS SHOWS FIREBRAND DISTRIBUTION IS NOT UNFORIM AND MORE PARTICLES HAVE LANDED ON POSITIVE X DIRECTION AND POSITIVE Y DIRECTION.

The firebrand generation number (70x5) and heat release rate are taken as inputs to quantify the firebrand and heat flux on the structure. The significance of this study is applying wind velocities of 3m/s, 6m/s and 12.5 m/s at 10 m height. After starting the simulation, it is being run for 60 seconds to obtain a quasi-steady wind field before initiating the ignition and firebrand generation. Figure 8 is the graphical representation of wind fields at -10 m and 0m after 60 seconds.

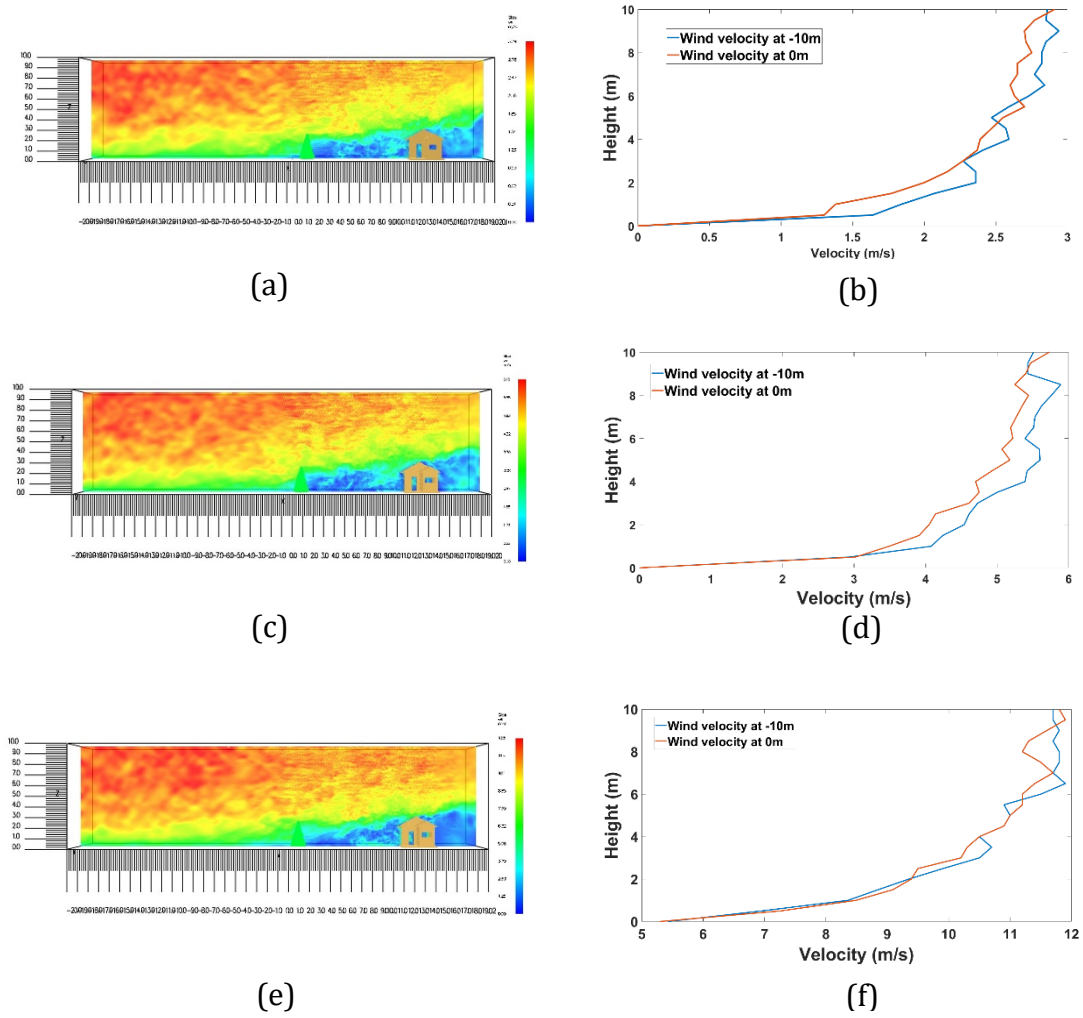

FIGURE 8(A), (C), (E) ILLUSTRATE THE SMOKEVIEW REPRESENTATIONS OF 3M/S, 6M/S AND 12.5 M/S WIND FLOW RESPECTIVELY. SYNTHETIC EDDY METHODOLOGY (SEM) IS USED TO INTRODUCE TURBULENCE AT THE DOMAIN INLET. THE VELOCITY PROFILES(3, 6, 12.5 M/S) AGAINST THE HEIGHT AT -10 M AND 0 M DISTANCE OF THE DOMAIN (10 M AND 20 M FROM THE INLET) ARE SHOWN IN (B), (D), (F).

Firebrand mass mass (kg) distribution contour maps in between the tree and house area are presented in Figure 9 (a), (b) and (c). The tree is located at (2, 0) on the XY plane and the house front wall is located at X=12 m. There is not much difference in firebrand mass distribution maps of 3 m/s and 6 m/s wind velocities. The maximum distance of firebrands transported is about 4 m in these wind speeds. But some firebrands have transported up to 8 m distance by 12.5 m/s wind velocity. The accumulation of firebrands at the bottom of the tree has reduced and spread more with the increase of the wind speed.

It is to be noted that, there is no firebrand that has reached the house in all three wind velocities. This is because of the low height of the tree (2.6 m) and the insufficiency of fire-induced buoyancy to lift the firebrands high enough to transport by the wind field.

These factors will be assessed in future simulations in terms of the height and a cluster of trees and the magnitude of fire to quantify firebrand and heat flux on the structure.

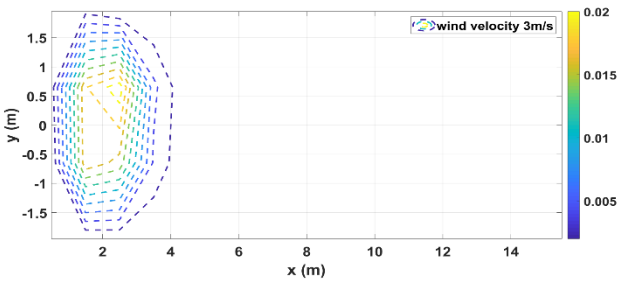

(a)

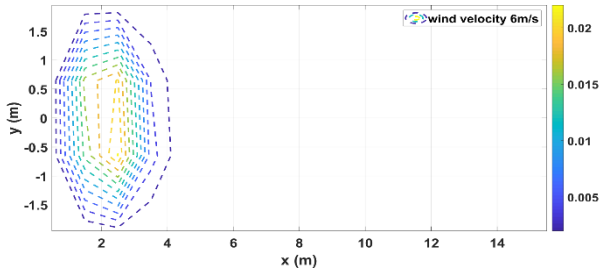

(b)

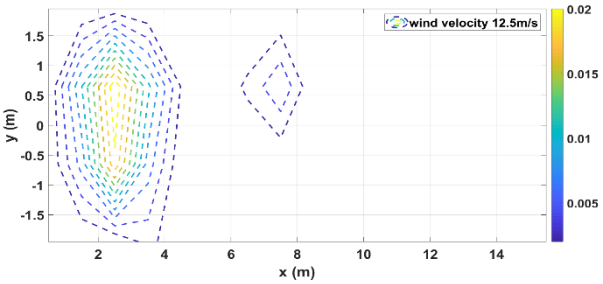

(c)

FIGURE 9 PRESENTS THE MASS (KG) DISTRIBUTION OF FIREBRANDS IN (A). 3 M/S (B). 6 M/S (C).12.5 M/S WIND VELOCITIES. INCREASING WIND VELOCITY UP TO 12.5 M/S SHOWS MORE FIREBRANDS MOVING TOWARDS RIGHT SIDE AND LESS ACCUMULATING WHERE THE TREE IS LOCATED.

Figure 10 is an illustration of firebrand landing on structures modelled in FDS [1]. A wind velocity of 13m/s, canopy height of 5m and, a static line fire with a magnitude of 18,640kW/m^2 were used there. It can be observed that a number of firebrand particles are landing on the structures under the influence of wind field, fire buoyancy and the elevation of the firebrand ejection in this particular event.

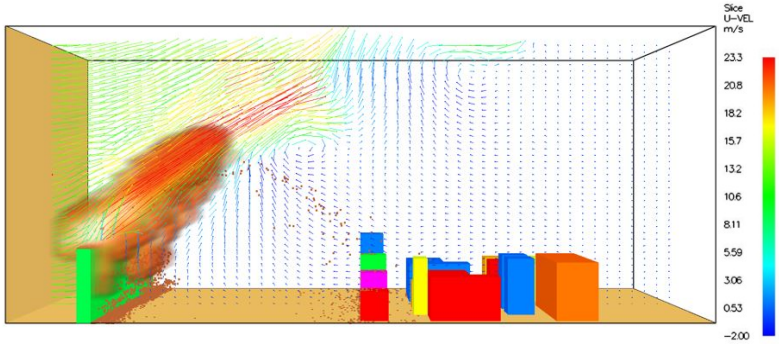

FIGURE 10 – A SMOKEVIEW REPRESENTATION OF FIREBRAND LANDING ON STRUCTURES MODELLED IN FDS. FIREBRANDS ARE RELEASED AT 5 M HIGH FROM THE GROUND LEVEL AND TRANSPORTED BY A 13 M/S WIND FIELD AND THE FIRE BUOYANCY [1].

The peak radiant heat flux obtained by different strategic locations (numbered 1 to 9) of the house at different driving wind velocities are computed and presented in Figure 11. The maximum radiant heat flux is observed at the centre of the front wall (2) which is the closest point to the tree burning location. The minimum radiant heat flux is observed at the door corner (4) which is not exposed much compared to other locations of the house.

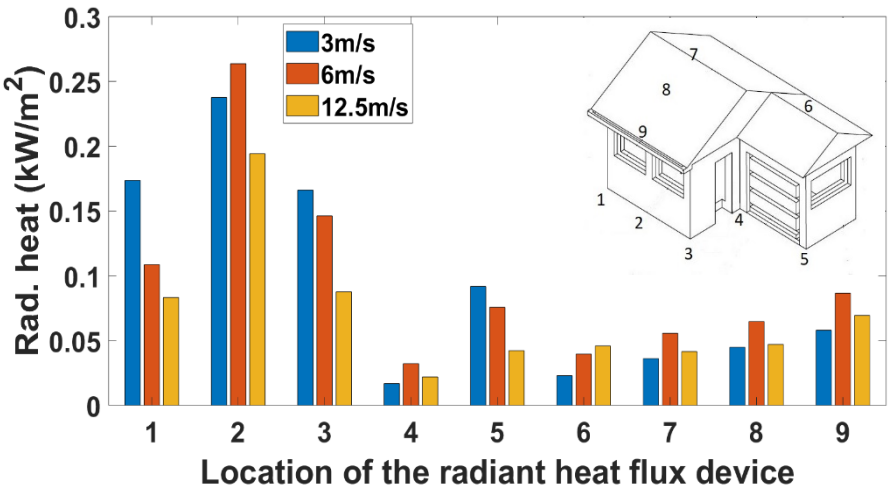

FIGURE 11 – LOCATION SPECIFIED PEAK RADIANT HEAT FLUXES OBTAINED BY THE EHAT FLUX DEVICES IN FDS FOR 3M/S, 6M/S AND 12.5M/S WIND VELOCITIES.

Flame height, temperature, and width are considered when computing the radiant heat flux in the AS3959 Standard. In the Standard, flame width is taken as arbitrarily as 100 m referring the length of the fire front [2]. The radiant heat flux is given as 40 kW/m2 at 10 m distance from the forest vegetation type for FDI 40 in AS3959. All computed peak radiant heat fluxes in these simulations are significantly less than predicted by AS3959. This is because of the low radiant heat emitted by burning a single tree instead of a 100 m wide fire line assumed in the AS3959.

CONCLUSIONS

The physics-based model FDS has been validated against the measurements from a single tree burning and firebrand distribution experiment conducted NIST. Firebrand data of the experiment were analyzed and divided into 30 mass classes to use as inputs to the model. It is to be noted that experimental firebrand collection was taken place by placing collection pans at strategic locations. For physics-based modelling, thermo-physical parameters were taken from previous studies of individual Douglas fir tree burning. The grid convergence of the model was appraised in terms of MLR and 50 mm grid size was found to be appropriate. An inverse analysis has been carried out to find the initial firebrand velocity and direction (as model inputs) to reach collection pans of all levels subject to the influence of fire-induced buoyancy and gravity forces. With this anlaysis, vertical and horizontal velocity components of 70 cm/s and 210 cm/s were taken as the initial velocities of firebrands generated by the burning tree. The firebrand generation number was examined inputting different multiplication (4, 5, 6, etc.) of experimental firebrand collection (70). The total mass of firebrands collected in the laboratory experiment was 18±4 g. Inputting 5□70 amount of firebrands in the simulation could obtain 18.9 g which is agree with the experiment.

Firebrand flux and heat load on the structure has been quantified for 3 m/s, 6 m/s and, 12.5 m/s wind speeds at 10 m above the ground in open field. Firebrand numbers, initial velocity and direction, tree geometry, and fuel composition were taken from the Douglas fir tree burning and firebrand transporting validation. Firebrand landing distribution (in terms of mass) contour maps show that increasing wind velocity results in transporting more firebrands towards the house and less accumulation at the bottom of the tree. But no firebrands landed on the house because of the low height of the tree and insufficiency of fire buoyancy to lift them high enough to transport by the wind. The heat flux devices of FDS at the ground level of the house and close to the tree burning location could obtain higher radiant heat flux compared to the locations on the roof. The AS3959 standard is based upon the radiant heat flux and BAL describes the heat flux permitted according to the distance between the fire and the structure. The computed radiant heat fluxes on the house in these simulations are significantly less than the standard. This will be examined further in future by simulating a cluster of taller trees (100 m wide) to quantify the heat flux and firebrand hazard on structures. The outcomes and key findings are expected to add to the prevailing AS3959 standard for the better counter the wildfire risk and improve the standards of building constructions in bushfire-prone areas.

REFERENCES

1 Amila Wickramasinghe, N.K., Khalid Moinuddin. Potential of modelling firebrand load on structure in Wildland Urban Interface in afac19. 2019. Melbourne: Bushfire and Natural Hazard CRC.
2 Australia, S., Construction of Buildings in Bush Fire Prone Areas (AS 3959). Standards Australia, Sydney, Australia, 2009.
3 Bryner, N.P., Building Codes and Standards for New Construction, in Encyclopedia of Wildfires and Wildland-Urban Interface (WUI) Fires, S.L. Manzello, Editor. 2018, Springer International Publishing: Cham. p. 1-9.
4 Manzello, S.L., et al., Mass and size distribution of firebrands generated from burning Korean pine (Pinus koraiensis) trees. Fire and Materials: An International Journal, 2009. 33(1): p. 21-31.
5 Ellis, P., The effect of the aerodynamic behaviour of flakes of jarrah and karri bark on their potential as firebrands. Journal of the Royal Society of Western Australia, 2010. 93: p. 21.
6 Alexander, M.E. and M.G. Cruz, Interdependencies between flame length and fireline intensity in predicting crown fire initiation and crown scorch height. International Journal of Wildland Fire, 2012. 21(2): p. 95-113.
7 Filkov, A., et al., Investigation of firebrand production during prescribed fires conducted in a pine forest. Proceedings of the Combustion Institute, 2017. 36(2): p. 3263-3270.
8 Manzello, S.L., S. Suzuki, and Y. Hayashi, Enabling the study of structure vulnerabilities to ignition from wind driven firebrand showers: A summary of experimental results. Fire Safety Journal, 2012. 54: p. 181-196.
9 Manzello, S.L., A. Maranghides, and W.E. Mell, Firebrand generation from burning vegetation1. International Journal of Wildland Fire, 2007. 16(4): p. 458-462.
10 Mell, W., et al., Numerical simulation and experiments of burning douglas fir trees. Combustion and Flame, 2009. 156(10): p. 2023-2041.
11 Mell, W., et al., Clarifying the meaning of mantras in wildland fire behaviour modelling: reply to Cruz et al.(2017). International journal of wildland fire, 2018. 27(11): p. 770-775.
12 Khan, N., et al., Physics-based simulation of heat load on structures for improving construction standards for bushfire prone areas. Frontiers in Mechanical Engineering, 2019. 5: p. 35.
13 Moinuddin, K. and D. Sutherland, Modelling of tree fires and fires transitioning from the forest floor to the canopy with a physics-based model. Mathematics and Computers in Simulation, 2019.
14 Mell, W.R., User Guide to WFDS. 2010, USA: National Institute of Standards and Technologies.
15 Kevin McGrattan, S.H., Randall McDermott, Jayson Floyd, Marcos Vanella, Fire Dynamics Simulator Technical Reference Guide. Vol. 1: Mathematical Model. 2019. 89.
16 FP-020, C., Australian Standard-Construction of buildings in bushfire prone areas. 2018: Sydney.
17 Engineering, T., Pyrosim User Manual. 2014.
18 McGrattan, K., et al., Fire dynamics simulator technical reference guide volume 1: mathematical model. NIST special publication, 2013. 1018(1): p. 175.
19 Technology, N.I.o.S.a., 2019.
20 Koo, E., et al., Modelling firebrand transport in wildfires using HIGRAD/FIRETEC. International journal of wildland fire, 2012. 21(4): p. 396-417.
21 Jarrin, N., et al., A synthetic-eddy-method for generating inflow conditions for large-eddy simulations. International Journal of Heat and Fluid Flow, 2006. 27(4): p. 585-593.